



Title	Quantitative analysis of defective sites in titanium(IV) oxide photocatalyst powders
Author(s)	Ikeda, Shigeru; Sugiyama, Noboru; Murakami, Shin-ya; Kominami, Hiroshi; Kera, Yoshiya; Noguchi, Hidenori; Uosaki, Kohei; Torimoto, Tsukasa; Ohtani, Bunsho
Citation	Physical Chemistry Chemical Physics, 5(4), 778-783 https://doi.org/10.1039/b206594k
Issue Date	2003
Doc URL	http://hdl.handle.net/2115/48674
Rights	Phys. Chem. Chem. Phys., 2003, 5, 778-783 - Reproduced by permission of the PCCP Owner Societies
Type	article (author version)
File Information	PCCP5_778.pdf



[Instructions for use](#)

Bunsho Ohtani

Catalysis Research Center, Hokkaido University, Sapporo 060-0811, Japan

TEL: +81-11-706-3673 FAX: +81-706-4925 E-mail: ohtani@cat.hokudai.ac.jp

Quantitative Analysis of Defective Sites in Titanium(IV) Oxide Photocatalyst Powders

Shigeru Ikeda,^{‡, †} Noboru Sugiyama,[†] Shin-ya Murakami,[§] Hiroshi Kominami,[§] Yoshiya Kera,[§] Hidenori Noguchi,[‡] Kohei Uosaki,[‡] Tsukasa Torimoto,^{‡, †} and Bunsho Ohtani^{*, ‡, †}

[‡] Catalysis Research Center, Hokkaido University, Sapporo 060-0811, Japan

[†] Graduate School of Environmental Earth Science, Hokkaido University, Sapporo 060-0810, Japan

[§] Department of Applied Chemistry, Faculty of Science and Engineering, Kinki University, Higashiosaka 577-8502, Japan

[‡] Graduate School of Science, Hokkaido University, Sapporo 060-0810, Japan

The molar amounts of defective sites (M_d) in several titanium(IV) oxide (TiO_2) powders were determined using photoinduced reaction of electron accumulation in deaerated aqueous solutions containing sacrificial hole scavengers and subsequent reduction of methylviologen to its cation radical. The measurements of pH dependence of typical anatase and rutile TiO_2 powders showed that these defective sites were of electronic energy just below the conduction band edge of TiO_2 in ranges of 0-0.35 V for anatase and 0-0.25 V for rutile. A linear relation of M_d with the rate constant of electron-hole recombination determined by femtosecond pump-probe diffuse reflection spectroscopy revealed that M_d could be a quantitative parameter of recombination between a

photoexcited electron and a positive hole. The tendency for M_d to increase, but not proportionally, with increase in the specific surface area suggested that these defective sites are mainly located near the external surfaces of TiO_2 particles. A reciprocal correlation between photocatalytic activity for water oxidation in aqueous silver sulfate solution and M_d revealed that the rate of recombination is one of the predominant physical properties governing the activities of TiO_2 powders in this reaction system.

Introduction

Polycrystalline titanium(IV) oxide (TiO_2) has been widely used as semiconductor photocatalysts in liquid-solid as well as in gas-liquid regimes¹⁻⁹ because of its sufficient photostability in various circumstances, nontoxicity for environments, and potent ability to induce various types of redox reactions.^{10,11} It is well known that photocatalytic activity strongly depends on bulk and surface physicochemical properties of the TiO_2 powder, such as the kind of crystal structure,¹²⁻¹⁵ surface area and particle size,¹⁶⁻²⁰ and surface hydroxyls.²¹⁻²³ Consequently, development of TiO_2 -photocatalytic systems with high efficiency by controlling the nature of TiO_2 is one of the most attractive targets of fundamental studies in this field.

A photocatalytic reaction is initiated by the generation of electron-hole (e^- - h^+) pairs by means of band-gap photoirradiation which can give rise to redox reactions with adsorbed species on the surface of the catalysis in competition with their disappearance due to mutual e^- - h^+ recombination. Thus, amount of adsorbed substrates and kinetic parameters for e^- - h^+ recombination, e.g., lifetime and rate constant, might also be important factors to control photocatalytic activities. Actually, in our previous studies,^{16,22,24-27} we have demonstrated that the overall rate of photocatalytic reactions in some liquid systems is governed by capture of electrons and positive holes by a surface adsorbed substrate(s) and e^- - h^+ recombination. Moreover, this implies that a highly

active TiO₂ photocatalyst should possess two properties simultaneously: a large surface area to absorb a substrate and a high degree of crystallinity (or few surface and bulk defects) to reduce e⁻-h⁺ recombination. This working hypothesis has been supported by highly active TiO₂ photocatalysts synthesized by a novel method, hydrothermal crystallization in organic media (HyCOM).^{7,28,29}

Compared with measurement of the amount of adsorbed substrates (or the specific surface area), measurement of kinetic parameters of e⁻-h⁺ recombination seems rather difficult, mainly due to the limitation of time resolution in conventional techniques. Electron paramagnetic resonance (EPR) spectroscopy has been used for detecting active species generated by photoirradiation of TiO₂ particles in the initial step of the photocatalytic reaction.³⁰⁻³⁵ These EPR studies have revealed that electrons are trapped on the surfaces and/or inside titanium atoms, thus forming Ti³⁺ species,³⁰⁻³⁴ while positive holes are trapped by oxygen atoms in the crystalline lattice and/or surface hydroxyl groups.^{32,34,35} Based on these findings, the reaction pathways of photocatalytic processes, especially for a photooxidation system, have been discussed and clarified in some aspects.³⁵

An alternative approach to determine e⁻-h⁺ behavior is to directly observe the dynamics of heterogeneous electron transfer on TiO₂ particles using ultrafast laser spectroscopy. Femtosecond pump-probe (PP) spectroscopy for TiO₂ particles and colloids³⁶⁻⁴³ has shown that certain surface sites trap electrons within a few tens of fs after the photoexcitation, giving a broad absorption at around 500-650 nm,^{44,45} and that their recombination with positive holes induces decay of absorption within 100 ps with second-order kinetics.^{39,40} By analyzing the decay kinetics of opaque TiO₂ powders measured in a diffuse reflection (DR) mode, we have proved that a kinetic parameter, rate constant of the absorption decay, could be a quantitative measure of the rate of e⁻-h⁺ recombination.^{40,41} Recently, reaction kinetics of trapped electrons in TiO₂ powders in a time domain from microseconds to milliseconds are also characterized by a

time-resolved IR absorption spectroscopy which allow to directly observe reaction kinetics of electron transfer from TiO₂ to substrates such as O₂ and H₂O.⁴⁶

One of the most important problems encountered to above mentioned spectroscopic techniques is the complexity of the measurement procedures for using as a general method for determining kinetic parameters of e⁻-h⁺ recombination. Our research interest has, therefore, been focused on developing an easy method other than above spectroscopic techniques for obtaining a quantitative measure of the rate of e⁻-h⁺ recombination. In the present study, the usefulness of a method for determining the molar amount of defective sites (M_d) of TiO₂ powder by means of photoinduced reaction of electron accumulation in TiO₂ in deaerated aqueous suspensions in the presence of a sacrificial hole scavenger was examined. Moreover, an example of correlation between photocatalytic activity and M_d was investigated.

Experimental Section

Materials. Several kinds of titanium oxide (TiO₂) powders, those from commercial sources (Degussa P-25, Merck, Ishihara CR-EL, and Hombikat UV-100), reference catalysts supplied from the Catalysis Society of Japan (JRC-TIO-1, -2, -3, and -5), and powders synthesized by the HyCOM method^{6,28,29} followed by a calcination at 1073 K under O₂ (designated as HyCOM(1073)), were used.

Measurement of the amount of accumulated electrons in photoirradiated TiO₂. A 50 mg portion of TiO₂ powder was suspended in an aqueous solution (5 cm³) containing a sacrificial hole scavenger, triethanolamine (TEOA, Wako Pure Chemical, 10 vol%) or methanol (Wako, 50 vol%), and the suspension was irradiated by a high-pressure mercury arc (Eiko-sha, 400 W) under argon (Ar). The photoirradiation was performed through a cylindrical Pyrex glass filter and a glass reaction tube (16 mm in diameter and 120 mm in length), so that light of wavelength > 300 nm reached the suspension. The

temperature of the suspension under photoirradiation was kept at 298 ± 0.5 K in a thermostatted water bath. After the irradiation, a deaerated aqueous solution (0.025 cm^3) of methylviologen (MV^{2+}) hydrochloride (Tokyo Kasei, $62.5\text{ }\mu\text{mol}$) was added to the photoirradiated suspension. The resulting pale blue suspension containing a reduced form of MV^{2+} , $\text{MV}^{\cdot+}$, was centrifuged and the supernatant solution was loaded in a quartz cell (light pass length, 1 mm) in an Ar purged glovebox (UN-650F, United Instruments). Absorbance of the solution at 600 nm was measured by a sensor array photometer (LASA 20, Toa Electronics), and the molar amount of $\text{MV}^{\cdot+}$ was determined using the reported value of the absorption coefficient of $\text{MV}^{\cdot+}$, $13700\text{ dm}^3\text{ mol}^{-1}\text{ cm}^{-1}$ at 606 nm.⁴⁷ It is noted that we could not measure the 606 nm absorbance due to the limitation of the acceptable wavelength to measure photoabsorption in our setup. However, in a separate experiment by means of an ultraviolet and visible light spectrophotometer (Hewlett Packard HP8453), we have confirmed that there is only negligible difference between the absorption coefficient of $\text{MV}^{\cdot+}$ at 606 nm and 600 nm.

In a separate experiment to quantify the amount of accumulated electrons by another chemical reaction, a deaerated aqueous solution containing colloidal platinum particles was added to the photoirradiated suspension under Ar instead of the addition of MV^{2+} . After shaking the mixture for a few minutes, the gas phase was analyzed using a gas chromatograph (GC, Shimadzu, GC-8A, equipped with an MS-5A column (GL Sciences) and a TCD detector).

PP-DR spectroscopy. Details of PP-DR spectroscopy were reported previously^{40,41} and are briefly summarized as follows. The light source consisted of a mode-locked Ti:sapphire laser (Spectra-Physics, Tsunami: 3960-L2S) pumped by an argon ion laser (Spectra-Physics, BeamLok: 2580C) with a regenerative amplifier system (Quantronix, 4812RGA/4823S/C), which was synchronously pumped by a mode-locked YLF laser

(Quantronix, 527DP-H). The final output was split into two beams with almost comparable intensities in order to pump two identical optical parametric generation (OPG)/optical parametric amplification (OPA) systems (Light Conversion, TOPAS). One output beam (620 nm) was used as a probe beam (1.5 mJ/pulse), and the other was frequency-doubled in a BBO crystal to use as a pump beam (0.1-0.03 mJ/pulse). The pump and probe beams were collinearly focused and overlapped at the sample, and the diffusely reflected probe beam was measured in air at ambient temperature. Reflectance data were accumulated and recorded as absorption, $1-R/R_0$, where R and R_0 represent the intensity at a given delay and that in the absence of a pump pulse, respectively.

Photoirradiation and product analyses. The photocatalyst (50 mg) and a 5 cm³ aqueous solution containing silver sulfate (Ag₂SO₄ (Wako Pure Chemicals), 50 mmol dm⁻³) were placed in a glass reaction tube (18 mm in diameter and 180 mm in length), and the suspension was photoirradiated (> 300 nm) under Ar with magnetic stirring (1000 rpm). The gaseous reaction product, O₂, was analyzed using a GC (Shimadzu, GC-8A, equipped with an MS-5A column and a TCD detector). Details of the procedure for the photocatalytic reaction and the product analysis were reported previously²².

Results and Discussion

Electron accumulation on TiO₂ powders.

Figure 1 shows the amounts of MV⁺· produced from photoirradiated P-25 and JRC-TIO-2 suspensions in deaerated aqueous TEOA (10%) solutions photoirradiated for various periods. When a deaerated aqueous MV²⁺ solution was injected into the aqueous suspension of TiO₂ after photoirradiation, a pale blue solution containing a reduced species of MV²⁺, MV⁺·, was obtained. On both TiO₂ powders, the amount of MV⁺· was saturated by extending the photoirradiation time for more than twenty hours,

though the times required for saturation to be completed in these two samples were different. It is also notable that there was an apparent difference in the saturated amounts of $MV^{+\cdot}$: $50 \mu\text{mol g}^{-1}$ on Degussa P-25 and $28 \mu\text{mol g}^{-1}$ on JRC-TIO-2. Similar behavior, saturation by photoirradiation for more than ca. twenty hours to different amounts of $MV^{+\cdot}$, was observed with other TiO_2 powders, suggesting that the amount of $MV^{+\cdot}$ depends on the nature of the TiO_2 powder. This speculation was supported by the dependence of the saturated $MV^{+\cdot}$ yield on the amount of TiO_2 . For example, the results for Degussa P-25 powder after 24 h of photoirradiation, which are shown in Fig. 2, show that a linear relation was obtained and that the slope, corresponding to the saturated amount of $MV^{+\cdot}$ per unit weight of the TiO_2 powder ($\mu\text{mol g}^{-1}$), was in good agreement with that obtained in the above-described time dependence shown in Fig. 1.

Figure 3 shows the time course of $MV^{+\cdot}$ production on JRC-TIO-2 powder in an aqueous methanol solution. The time course in a TEOA solution plotted in Fig. 1 is also shown for comparison. Similar to the case of TEOA, the $MV^{+\cdot}$ production was also saturated by photoirradiation for more than ca. 35 h when methanol was used. However, even though the same TiO_2 powder was used, the saturated $MV^{+\cdot}$ amount in methanol solution is obviously less than that obtained in the TEOA solution. On the other hand, almost the same amount of $MV^{+\cdot}$ was produced by both hole-scavengers when pH of the methanol solution was fixed at ca. 11, which is almost the same as that of the TEOA solution (pH = ca. 10.5), and photoirradiated for 60 h. These results indicate that the amount of accumulated $MV^{+\cdot}$ depends on pH of the solution but is not influenced by the nature of hole-scavengers. In order to examine in detail the influence of pH on $MV^{+\cdot}$ production, two sets of experiments were carried out using two kinds of TiO_2 powders with different crystal structures. In one set of experiments, photoirradiation was conducted at pH of ca. 11 for 40 h in the presence of TEOA or methanol, and deaerated H_2SO_4 was added after the photoirradiation in order to control pH of the solution. In the other set of experiments, photoirradiation was conducted at pH of ca. 2 for 40 h, and

deaerated NaOH was added after the photoirradiation. The results are shown in Fig. 4. When JRC-TIO-2, consisting of anatase crystallites, was used, the amount of $MV^{\cdot+}$ was significantly different at pH of around 2-8 in both sets of experiments; almost no $MV^{\cdot+}$ was produced at pH lower than 2, but the amount produced gradually increased with increase in pH. On the other hand, the pH dependence of CR-EL, mostly rutile crystallites, was much sharper than that of the anatase (JRC-TIO-2); a jump in $MV^{\cdot+}$ yield was observed at pH ca. 8-10. Anyway, the agreement of pH dependencies in the two sets of experiments suggests that the dependence of pH is only due to the difference in pH during the reduction of MV^{2+} , and there is no significant affect of additives such as NaOH and/or H_2SO_4 on the present results.

When light with energy greater than the band-gap of TiO_2 is irradiated on a deaerated aqueous TiO_2 suspension containing sacrificial hole scavengers in the absence of loaded effective catalyst deposits for water reduction such as platinum, a part of TiO_2 particle is converted by photoexcited electrons into a reduced species of Ti^{4+} (Ti^{3+}), i.e., electrons accumulate in some states of TiO_2 in the form of Ti^{3+} . As mentioned in the introduction section, these Ti^{3+} species have been detected by EPR spectroscopy.³⁰⁻³⁴ The formation of Ti^{3+} is also indicated by the change in color from white to blue during the photoirradiation. At present, though the detailed structures of these Ti^{3+} species are not clear, it is reasonable to assume that such Ti^{3+} species are produced by trapping of electrons at defective sites in TiO_2 , and the amount of accumulated electrons may therefore reflect the number of defective sites that work presumably as recombination sites of e^- and h^+ . When a deaerated aqueous $MVCl_2$ (MV^{2+}) solution is added to this suspension containing Ti^{3+} , MV^{2+} can be reduced by such accumulated electrons.



As shown in Fig. 4, in the lower pH region where negligible production of $MV^{\cdot+}$ was

observed with both TiO₂ suspensions, the blue color of TiO₂ was unchanged, i.e., the electron transfer given by eq. (1) did not proceed. At higher pH (pH > 2 for anatase TiO₂ and pH > 8 for rutile), however, the color of TiO₂ particles changed to white, and a pale blue solution was obtained by the addition of MV²⁺. The amount of MV⁺· was saturated, resulting in a plateau in the MV⁺·-versus-pH curve at pH higher than 8 for anatase or 10 for rutile due to the elimination of electrons accumulated in defective sites of TiO₂ powder by complete electron transfer to MV²⁺, i.e., equimolar amounts of Ti³⁺ and MV²⁺ reacted to produce MV⁺· at pH higher than 10, corresponding to the pH of the 10 vol% aqueous TEOA solution used in the first experiment as shown in Fig. 1. Therefore, the amount of MV⁺· produced in TEOA solution is considered to reflect the molar amount of defective sites (M_d) of TiO₂ powder, which should be an inherent value dependent on the nature of TiO₂.

For the spontaneous electron transfer from the defective site of Ti³⁺ to MV²⁺ as depicted in eq. (1), at least the electrochemical potential of the defective sites requires to be more negative than the energy level of MV²⁺/ MV⁺· redox couple (E_{MV}). Thus, the observed pH dependencies of MV⁺· production suggest that the energy level of Ti³⁺ species have pH dependence, i.e., the position of electrochemical potential of defective sites in higher pH region (pH > 8 for anatase or > 10 for rutile) is relatively negative as compared to the energy level of MV²⁺ but that in lower pH region (pH < 2 for anatase or < 8 for rutile) is reversed. Assuming that negligible activation energy is required to drive the electron transfer from Ti³⁺ to MV²⁺, the molar amount of produced MV⁺· (M_{MV+}, μmol g⁻¹) at given pH corresponds to the amount of defective sites of energy level between conduction band edge of TiO₂, which is identical to flat band potential of TiO₂ (E_{fb}), and E_{MV}. E_{fb} and E_{MV} are given by the following Nernst equation:

$$E_{fb} = E_{fb}^0 - 0.059 \text{ pH} \quad (\text{V vs NHE}), \quad (2)$$

$$E_{MV} = E_{MV}^0 - 0.059 \log ([MV^{+}]/[MV^{2+}]) \quad (\text{V, vs NHE}), \quad (3)$$

where E_{fb}^0 and E_{MV}^0 represent the flat band potential of TiO_2 powders at pH 0 (E_{def}^0 , -0.20 V for anatase and +0.04 V for rutile (vs NHE))⁵¹ and the equilibrium potential of MV^{2+}/MV^{+} redox couple (-0.45 V vs NHE),⁵² respectively. The application of eq. (3) for the expression of E_{MV} includes the assumption that the reduction of MV^{2+} by Ti^{3+} given in eq. (1) is a reversible reaction. The difference between E_{fb} and E_{MV} is described as

$$E = E_{MV} - E_{fb} = -0.45 - 0.059 \log ([MV^{+}]/[MV^{2+}]) - E_{fb}^0 + 0.059 \text{ pH}. \quad (4)$$

Accordingly, the observed pH dependences on both anatase and rutile TiO_2 particles (Fig. 4) can be expressed as amount of MV^{+} production ($M_{MV^{+}}$) at different potentials between E_{fb} and E_{MV} , which are shown in Fig. 5. Since E can be regarded as the potential normalized by E_{fb} as a zero standard and $M_{MV^{+}}$ reflects the density of defective sites ($M_d(E)$, $\mu\text{mol g}^{-1} \text{ V}^{-1}$) between E_{fb} and E_{MV} , it is clear that defective sites are distributed just below the conduction band edges of TiO_2 (E_{cb}) and expressed as following equation:

$$M_{MV^{+}} = \int_0^{E_{MV} - E_{fb}} M_d(E) dE. \quad (5)$$

A differential of eq. (5),

$$M_d(E) = dM_{MV^{+}}/dE, \quad (6)$$

indicates that the density of defective sites is directly proportional to the derivative of amount of MV^{+} production ($dM_{MV^{+}}/dE$), which provides a direct measure of the

distribution of defective sites. Plots of dM_{MV^+}/dE vs E , which were obtained by calculating dM_{MV^+}/dE , are shown in the insert of Fig. 5. In the anatase TiO_2 (JRC-TIO-2), a relatively broad distribution of defective sites in a range of electric energy of ca. 0-0.35 V below E_{cb} was obtained in comparison with the distribution in the rutile TiO_2 (CR-EL) (ca. 0-0.25 V below E_{cb}). Furthermore, it should be noted that the observed distributions in both TiO_2 's are shallower than that of a polycrystalline TiO_2 electrode determined by an electrochemical technique (ca. 0.2-0.4 V below E_{cb}).⁵⁰ Although further investigations are necessary to understand the predominant factor leading to these different distributions, these results suggest that the electric energy of defective sites strongly depends on the kind and/or nature of TiO_2 particles.

According to the proposed reaction of eq. (1), it is expected that other reagents or reactions are also applicable for measuring the amount of Ti^{3+} . In order to confirm this, the reduction of proton (H^+) catalyzed by the addition of a platinum colloid catalyst was carried out instead of the MV^{2+} reduction.



When P-25 was used, for example, the liberation of 1.2 μ mol of H_2 per 50 mg of TiO_2 , which is almost half that of MV^+ , was liberated. Thus, the observed MV^+ production was induced by the accumulated electrons in defective sites of TiO_2 powders, and the amount of these defective sites could be quantified by the chemical reactions.

Correlation with other physical properties and photocatalytic activity. Figure 6 shows representative time profiles of Merck TiO_2 powder in PP-DR spectroscopy. When a 310-nm light beam (ca. 100 fs pulse) was irradiated onto TiO_2 powders, broad absorption in the visible-infrared region (In this system, diffuse reflected light at 620 nm was measured.) appeared and was decreased with increased time delay of the probe

pulse at 620 nm.⁴⁰⁻⁴³ All of the TiO₂ samples studied here showed similar decay profiles consisting of very rapid (< ca. 250 fs) rise in absorption at 620 nm and its gradual decay. The decay profiles could be reproduced by a second-order rate expression using the equation

$$(\text{absorption}) = \alpha \{ [e_0] / (1 + k_r [e_0] t) + \text{BL} \}, \quad (8)$$

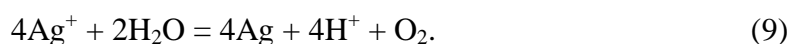
where $[e_0]$, k_r , t , and BL represent the initial concentration of trapped electrons, second-order rate constant ($\text{cm}^3 \text{ps}^{-1}$), time delay of the probe pulse (ps), and a component of the long-lived baseline, respectively. The parameter α (cm^3) includes a photoabsorption cross section of the components and depth of penetration of the pump pulse and must vary with the measurement conditions. As has been discussed,^{40,41} k_r ($\text{cm}^3 \text{ps}^{-1}$) values of TiO₂ powders were determined with the assumption that α equals unity for every sample. Table 1 summarises k_r and other parameters, molar amounts of defective sites (M_d , $\mu\text{mol g}^{-1}$), BET surface areas (S , $\text{m}^2 \text{g}^{-1}$), and photocatalytic activity for O₂ liberation from deaerated aqueous silver sulfate solution as discussed below.

As shown in Fig. 7, an almost linear correlation of k_r with M_d of several TiO₂ powders was observed. It is noted that there seems no specific influence on the difference of crystal structure, e.g., anatase, rutile, and their mixtures. Although details of the mechanism of e^-h^+ recombination on TiO₂ photocatalysis is not clear, if it is assumed that the predominant pathway of recombination in both anatase and rutile TiO₂ is that of photoexcited electrons with positive holes at defective sites, a linear relation between these parameters is reasonable. Therefore, it is concluded that M_d can be a quantitative kinetic measure of the e^-h^+ recombination.

Figure 8 shows plots of M_d as a function of S . M_d tended to increase with increase in S , implying that the electron accumulation sites, defective sites, mainly exist near the external surface of TiO₂ particles. The number of Ti atoms on the external

surface of JRC-TiO-2, for example, is estimated to ca. 210 $\mu\text{mol g}^{-1}$, while M_d on this TiO_2 powder is 28 $\mu\text{mol g}^{-1}$ (Fig. 1); it is reasonable to assume the existence of such electron accumulation sites on the surface. Although the detailed structure is still ambiguous as mentioned above, such electron accumulation on defective sites seem to be accompanied by surface sites on TiO_2 powders and the excess negative charge may be compensated by the insertion of protons (H^+) from the aqueous phase^{53,54}, and/or elimination of O^{2-} ions.

Previous studies have indicated that the stoichiometry of the main reactions in an aqueous suspension of TiO_2 in the presence of silver ions under deaerated condition was as follows:²²



Consequently, we could estimate the overall rate of redox reaction by the rate of O_2 liberation from its time-course curve during the initial 0.5 h of photoirradiation (Table 1). Figure 9 shows a plot of photocatalytic activity versus M_d . The rate of the reaction tended to decrease with increasing M_d , suggesting that the rate of e^-h^+ recombination might predominantly govern photocatalytic activity of this reaction, agreed well with our previous kinetic analyses.²² Therefore, it is considered that a TiO_2 powder having relatively high crystallinity, low amount of defective sites, is appropriate in this type of reaction. On the other hand, it is also notable that some of TiO_2 powders (JRC-TiO-2, Merck) are fairly deviated from the inversed-proportional-curve of the correlation. The specific feature of these powders might be attributed to the crystal structure, i.e., anatase TiO_2 is not active for this photocatalytic reaction, and thus it is speculated that a rutile TiO_2 having high crystallinity might be the most suitable photocatalyst for this type of reaction. In order to clarify the influence of the crystalline phase, detailed studies are now under way, and the results will be reported elsewhere.⁵⁵

Conclusions

A simple method to determine the amount of defective sites of a TiO₂ powder photocatalyst has been developed. These defective sites were of electronic energy just below the conduction band edge of TiO₂ in ranges of 0-0.35 V for a typical anatase and 0.-0.25 V for a typical rutile TiO₂ powders. An almost linear relation of M_d with the rate constant of electron-hole recombination revealed that M_d could be a quantitative measure of recombination. By analyzing the correlation with photocatalytic activity for water oxidation in the presence of silver ions, it was clarified that M_d was the predominant factor determining the photocatalytic activity of TiO₂. Such correlations between photocatalytic activity and physical properties might be a specific feature of this kind of reaction, and predominant physical properties should be different among types of photocatalytic reactions. Accordingly, in order to design and predict efficient TiO₂ photocatalysts in a desired reaction system, it is necessary to choose appropriate parameters of TiO₂ powder.

Acknowledgements

The authors are grateful to the Catalysis Society of Japan for supplying some of the TiO₂ samples. This research was partly supported by Grant-in-Aids for Encouragement of Young Scientists (No. 13750753) and for Scientific Research on Priority Areas (417, No. 14050007) from the Japan Society for the Promotion of Science (JSPS) and the Ministry of Education, Culture, Sports, Science and Technology (MEXT) of the Japanese Government, respectively. Financial support by The Sumitomo Foundation is acknowledged. Mr. Tetsuzo Habu and Mr. Kazuhiro Matsudaira (Technical Division of the Catalysis Research Center, Hokkaido University) are acknowledged for their assistance in the construction of the photoirradiation apparatuses.

References

1. M. R. Hoffmann, S. T. Martin, W. Choi and D. W. Bahnemann, *Chem. Rev.*, 1995, **95**, 69.
2. A. L. Linsebigler, G. Lu and J. T. Yates, *Chem. Rev.*, 1995, **95**, 735.
3. A. Fujishima, K. Hashimoto and T. Watanabe, in *TiO₂ Photocatalysis - Fundamentals and Applications*, BKC, Tokyo, 1999, 176.
4. *Energy Resources through Photochemistry and Catalysis*, ed. M. Grätzel, Academic Press, New York, 1983.
5. S. Tabata, H. Nishida, Y. Masaki and K. Tabata, *Catal. Lett.*, 1995, 34.
6. H. Kominami, S.-y. Murakami, M. Kohno, Y. Kera, K. Okada, and B. Ohtani, *Phys. Chem. Chem. Phys.*, 2001, **3**, 4102.
7. R. Abe, K. Sayama, K. Domen and H. Arakawa, *Chem. Phys. Lett.*, 2001, **344**, 339.
8. M. A. Fox and M. T. Dulay, *Chem. Rev.*, 1993, **93**, 341.
9. B. Ohtani, S. Kusakabe, K. Okada, S. Tsuru, S.-i. Nishimoto, Y. Amino, K. Izawa, Y. Nakato, M. Matsumura, Y. Nakaoka and Y. Nosaka, *J. Chem. Soc., Perkin Trans. 2*, 2001, 201.
10. A. Mills and P. Sawunyama, *J. Photochem. Photobiol. A: Chem.*, 1997, **108**, 1.
11. *Heterogeneous Photocatalysis*, ed. M. Schiavello, John Wiley & Sons, Chichester, 1997.
12. A. Mills, R. H. Davies and D. Worsley, *Chem. Soc. Rev.*, 1993, 417.
13. S.-i. Nishimoto, B. Ohtani, H. Kajiwara and T. Kagiya, *J. Chem. Soc., Faraday Trans. 1*, 1985, **81**, 61.
14. R. I. Bickley, T. Gonzalez-Carreno, J. S. Lees, L. Palmisano and R. J. D. Tilley, *J. Solid State Chem.*, 1991, **92**, 178.
15. M. V. Rao, K. Rajeswar, V. R. Pai Verneker and J. DuBow, *J. Phys. Chem.*, 1980,

- 84**, 1987.
16. B. Ohtani, S.-w. Zhang, S.-i. Nishimoto, and T. Kagiya, □*J. Photochem. Photobiol., A: Chem.*, 1992, **64**, 223.
 17. T. Sakata, T. Kawai and K. Hashimoto, □*Chem. Phys. Lett.*, 1982, **88**, 50.
 18. B. Ohtani, J.-i. Handa, S.-i. Nishimoto and T. Kagiya, □*Chem. Phys. Lett.*, 1985, **120**, 292.
 19. A. Sclafani, L. Palmisano and M. Schiavello, □*J. Phys. Chem.*, 1990, **94**, 829.
 20. K. Tanaka, M. F. V.Capule and T. Hisanaga, □*Chem. Phys. Lett.*, 1991, **187**, 73.
 21. Y. Oosawa and M. Grätzel, □*J. Chem. Soc., Chem. Commun.*, 1984, 1629.
 22. B. Ohtani, Y. Okugawa, S.-i. Nishimoto and T. Kagiya, □*J. Phys. Chem.*, 1987, **91**, 3550.
 23. Y. Oosawa and M. Grätzel, □*J. Chem. Soc., Faraday Trans. 1*, 1988, **84**, 197.
 24. S.-i. Nishimoto, B. Ohtani, H. Kajiwara and T. Kagiya, □*J. Chem. Soc., Faraday Trans. 1*, 1983, **79**, 2685.
 25. B. Ohtani, M. Kakimoto, H. Miyadzu, S.-i. Nishimoto and T. Kagiya, □*J. Phys. Chem.*, 1988, **92**, 5773.
 26. B. Ohtani and S.-i. Nishimoto, □*J. Phys. Chem.*, 1993, **97**, 920.
 27. B. Ohtani, K. Tennou, S.-i. Nishimoto and T. Inui, □*J. Photosci.* 1995, **2**, 7.
 28. H. Kominami, T. Matsuura, K. Iwai, B. Ohtani, S.-i. Nishimoto and Y. Kera, □*Chem. Lett.*, 1995, 693.
 29. B. Ohtani, K. Iwai, H. Kominami, T. Matsuura, Y. Kera and S.-i. Nishimoto, *Chem. Phys. Lett.*, 1995, **242**, 315.
 30. R. F. Howe and M. Grätzel, *J. Phys. Chem.*, 1985, **89**, 4495.
 31. R. F. Howe and M. Grätzel, *J. Phys. Chem.*, 1987, **91**, 5889.
 32. O. I. Micic, Y. Zhang, K. R. Cromack, A. D. Trifunac and M. C. Thurnauer, □*J. Phys. Chem.*, 1993, **97**, 13284.
 33. J. Kiwi, J. T. Suss and S. Szapiro, □*Chem. Phys. Lett.*, 1984, **106**, 135.

34. Y. Nakaoka and Y. Nosaka, *J. Photochem. Photobiol., A: Chem.*, 1997, **110**, 299.
35. Y. Nosaka, M. Kishimoto and J. Nishino, *J. Phys. Chem. B.*, 1998, **102**, 10279.
36. D. E. Skinner, D. P. Colombo Jr., J. J. Cavaleri and R. M. Bowman, *J. Phys. Chem.*, 1995, **99**, 7853.
37. D. P. Colombo Jr. and R. M. Bowman, *J. Phys. Chem.*, 1995, **99**, 11752.
38. D. P. Colombo Jr., K. A. Roussel, J. Saeh, D. E. Skinner, J. J. Cavaleri and R. M. Bowman, *Chem. Phys. Lett.*, 1995, **232**, 207.
39. D. P. Colombo Jr. and R. M. Bowman, *J. Phys. Chem.*, 1996, **100**, 18445.
40. B. Ohtani, H. Kominami, R. M. Bowman, D. P. Colombo Jr., H. Noguchi and K. Uosaki *Chem. Lett.*, 1998, 579.
41. S. Ikeda, N. Sugiyama, B. Pal, G. Marci, L. Palmisano, H. Noguchi, K. Uosaki and B. Ohtani, *Phys. Chem. Chem. Phys.*, 2001, **3**, 267.
42. A. Furube, T. Asahi, H. Masuhara, H. Yamashita and M. Anpo, *Chem. Lett.*, 1997, 735.
43. A. Furube, T. Asahi, H. Masuhara, H. Yamashita, M. Anpo, *J. Phys. Chem. B.*, 1999, **103**, 3120.
44. G. Rothenberger, J. Moser, M. Grätzel, N. Serpone, N. and D. K. Sharma, *J. Am. Chem. Soc.*, 1985, **107**, 8054.
45. N. Serpone, D. Lawless, R. Khairutdinov, *J. Phys. Chem.*, 1995, **99**, 16655.
46. A. Yamakata, T.-a. Ishibashi and H. Onishi, *J. Phys. Chem. B.*, 2001, **105**, 7258.
47. T. Watanabe and K. Honda, *J. Phys. Chem.*, 1982, **86**, 2617.
48. H. Kominami, J.-i. Kato, M. Kohno, Y. Kera and B. Ohtani, *Chem. Lett.*, 1996, 1051.
49. S.-i. Nishimoto, B. Ohtani, H. Kajiwara and T. Kagiya, *J. Chem. Soc., Faraday Trans. 1*, 1985, **81**, 2467.
50. H. Wang, J. He, G. Boschloo, H. Lindström, A. Hagfeldt, S.-E. Lindquist, *J. Phys. Chem. B*, 2001, **105**, 2529, and references are therein.

51. L. Kavan, M. Grätzel, S. E. Gilbert, C. Klemenz and H. J. Scheel, *J. Am. Chem. Soc.*, 1996, **118**, 6716.
52. A. J. Bard, in *Standard Potentials in Aqueous Solution*, ed. M. Delder, New York; 1985, 49.
53. B. I. Lemon and J. T. Hupp, *J. Phys. Chem.*, 1996, **100**, 14578.
54. B. I. Lemon and J. T. Hupp, *J. Phys. Chem.*, 1997, **101**, 2426.
55. T. Torimoto, N. Nakamura, S. Ikeda and B. Ohtani, to be published.

Figure Captions

Fig. 1. Plots of molar amount of $MV^{+\cdot}$ versus photoirradiation time. Upper, Degussa P-25; lower, reference TiO_2 catalyst, JRC-TIO-2, supplied by the Catalysis Society of Japan.

Fig. 2. Plots of molar amount of $MV^{+\cdot}$ as a function of amount of TiO_2 powder. Catalyst, Degussa P-25; photoirradiation time, 24 h. Slope denotes molar amount of $MV^{+\cdot}$ per unit weight of the catalyst powder.

Fig. 3. Plots of molar amount of $MV^{+\cdot}$ from a deaerated aqueous solution of TEOA (A) and methanol (B) versus photoirradiation time. Open circles, TEOA aq. (pH = ca. 10.5); filled diamonds, methanol aq. (pH = ca. 7.0); open diamonds, methanol aq. (pH = ca. 11.0). Catalyst, JRC-TIO-2.

Fig. 4. Dependence of the amount of $MV^{+\cdot}$ production on solution pH. Upper, anatase TiO_2 (JRC-TIO-2); lower, rutile TiO_2 (CR-EL). Open squares, photoirradiation at pH of ca. 11; filled squares, photoirradiation at pH of ca. 2.

Fig. 5. The amount of $MV^{+\cdot}$ production at different potentials based on the flat band potential of TiO_2 . Upper, anatase TiO_2 (JRC-TIO-2); lower, rutile TiO_2 (CR-EL). The inserts show $dM_{MV^{+\cdot}}/dE$ distribution against potentials. The meanings of symbols are the same as those in Fig.4.

Fig. 6. Representative decay profiles of TiO₂ powders induced by an ultrafast pump (ca. 100 fs). Sample, Merck TiO₂. Solid line indicates the fitting with eq. (8).

Fig. 7. Relation between M_d and k_r. (a) Degussa P-25, (b) Merck, (c) JRC-TIO-2, (d) JRC-TIO-5, (e) HyCOM(1073). Open circles, filled circles, and filled diamonds denote anatase, rutile, and their mixtures, respectively.

Fig. 8. Relation between S and M_d. (a) Degussa P-25, (b) Merck, (c) JRC-TIO-2, (d) JRC-TIO-5, (e) HyCOM(1073), (f) UV-100, (g) CR-EL, (h) JRC-TIO-1, (i) JRC-TIO-3. The meanings of symbols are the same as those in Fig.7.

Fig. 9. Rate of O₂ evolution on several TiO₂ powders versus M_d. The meanings of characters and symbols are the same as those in Fig.'s 7 and 8.